

Reaction of a Mo Atom with H₂, N₂, and O₂: A Density Functional Study

Ana Martínez,[†] Andreas M. Köster,[‡] and Dennis R. Salahub*

Département de Chimie, Université de Montréal, C. P. 6128, Succursale Centre-Ville, Montréal, Québec H3C 3J7, Canada

Received: June 21, 1996; In Final Form: November 22, 1996[⊗]

The reactivity of a Mo atom with H₂, N₂, and O₂ is investigated with the all-electron Linear Combination of Gaussian Type-Orbitals–Kohn–Sham–Density Functional Theory (LCGTO-KS-DFT) method. We used MoH₂ to validate the DFT methodology, comparing with accurate relativistic CI results. After this validation we studied the reaction of a Mo atom with N₂ and O₂ in order to obtain an explanation of the different observed reactivities. The equilibrium geometries are characterized by their binding energies, electronic states, and harmonic frequencies. For MoN₂ we found two local minima under the dissociation limit on the quintet surface that are very weakly bonded. For MoO₂ we found several local minima on different potential energy surfaces. The lowest minimum for this system is a bent structure on the triplet potential energy surface. A detailed analysis of the molecular orbitals is given. We suggest a two-step charge transfer process as the mechanism of the reaction, and we found that the Mo atom is always the electron donor. The theoretical explanation of the experimental results provide a better understanding of the electronic structure and the reaction mechanism.

Introduction

The reactivity of small metal clusters is a topic of major interest because these clusters can be used as models in the study of the reactivity of metal centers in catalytic processes. For example, the fixation of nitrogen, a very important process in nature and in industry, always requires a transition metal as a catalyst. The biological catalyst (the nitrogenase enzyme) contains Mo and Fe atoms. In the industrial process for the synthesis of ammonia from N₂ and H₂ (Haber–Bosch process), an Fe metal catalyst is used. The study of N₂ chemisorption on transition metal clusters provides a possibility to improve our understanding of the factors that influence nitrogen fixation. The investigation of physisorption and chemisorption on clusters, as well as the incorporation of atoms and molecules into clusters,^{1–5} has become possible due to the spectacular progress in cluster research. The developments of both theory and experiments will provide more knowledge of many properties of atomic aggregates.

One of the most important questions about the behavior of clusters is the change in reactivity as a function of cluster size. Particularly, the reactivity of transition metal clusters reveals a dramatic size dependence.^{6,7} Lian *et al.*⁸ reported an experimental study using resonance fluorescence excitation, found significant differences in the reactivity of Mo atoms and clusters. For example, Mo atoms and dimers show no reaction with H₂ and N₂, whereas both react with O₂ spontaneously. Mo atoms react with C₂H₄ but do not react with NH₃, while Mo dimers present the reverse behavior. On the other hand, Mo₃ has a great reactivity with N₂.⁹ They discussed the possible origins of this behavior using the valence electronic structures of Mo and Mo₂, and reported that dimers and clusters have mechanisms for reducing repulsive interactions that are not available to atoms. In order to find the link between electronic structure and reactivity, it is necessary to perform reliable electronic structure calculations. In this paper we will focus on the low-

lying electronic states of MoL₂ where L₂ is a diatomic homonuclear molecule. Related work on small clusters will be reported elsewhere.

There are many theoretical works about the reaction of transition metal atoms with the hydrogen molecule.^{10–22} The theoretical information about these systems can be summarized in the following points. First, it is necessary to include electron correlation, when the problem of the dissociation of H₂ is studied. Second, the metal atom is more able to react if it is present in the d^{*n*–1}s¹ configuration than in the d^{*n*–2}s² configuration. Third, there are two possible bonding situations, bent (C_{2v} symmetry) and linear (C_{∞v} symmetry) structures. For the bent complexes, the formation of “sd” hybrid bonds is important. In both complexes, the “d” orbitals play an important role in the dissociation reaction. Fourth, relativistic effects may influence the strength of the M–H bond (for example, when the comparison between Pd and Pt is made), and fifth, the reaction is different when the metal atom is ionized. All these factors are also important for reactions on Mo atom clusters. Recently, Li and Balasubramanian¹⁸ reported the electronic states and the potential energy surfaces of Mo with H₂. They performed complete active space MCSCF (CASSCF) followed by multireference singles and doubles configuration interaction (MRSDCI) calculations, and they also include the relativistic CI (RCI) method. They found that the ground state of the MoH₂ molecule is a ⁵B₂ bent state, with an Mo–H bond distance of 1.67 Å and an H–Mo–H bond angle of 116°.

In this work, in order to validate our methodology, we present a nonrelativistic density functional study of the interaction of the Mo atom with H₂. As we will see later, our results are in good agreement with the above CI results for the properties and relative energies of the various local minima involved. Relativistic effects are not crucial for the qualitative description of these species (although, as discussed in ref 18, spin–orbit coupling provides a mechanism for hopping between states of different multiplicities in the surface crossing region).

For the reaction of N₂ with transition metals, the experimental information of particular relevance can be summarized in two points. The first is that the dissociation of N₂ with small or no energy barriers is only possible with metals that have open d orbitals. The second point establishes that Fe and Cr are able

[†] Permanent address: Departamento de Química, División de Ciencias Básicas e Ingeniería, Universidad Autónoma Metropolitana-Iztapalapa, A. P. 55–534, México D. F. 09340, México.

[‡] Permanent address: Theoretische Chemie, Universität Hannover, Am Kleinen Felde 30, 30167, Hannover, Germany.

[⊗] Abstract published in *Advance ACS Abstracts*, January 15, 1997.

to dissociate N₂, whereas Ni and Co do not present dissociative reactions. The difference between different metals in their ability to react with N₂ must be explained with a systematic study of the electronic structures of the metal and the molecule. Following this idea, Siegbahn and Blomberg²³ performed a theoretical study using the complete active space self consistent field method, followed by a multireference contracted CI calculations. They reported that the more stable structures are in the end-on approach, in agreement with most of the metal complexes that are well characterized experimentally. Bauschlicher *et al.*²⁴ reported a CASSCF study of FeN₂, FeCO, and Fe₂N₂. They found similar reactivity behavior of N₂ and CO in the side-on bonding geometry.

As we pointed out before, Lian *et al.*⁸ reported a very detailed experimental study about the reaction of the Mo atom and dimer with several small molecules. In order to explain the behavior of the Mo atoms with some of those molecules, we have performed a density functional study of the interaction of the Mo atom with H₂, N₂, and O₂. After validating our methodology on MoH₂, we studied MoN₂ and MoO₂ in order to obtain an explanation of the different reactivity behaviors. We report bond distances, equilibrium geometries, binding energies, electronic states, and harmonic frequencies for MoH₂, MoN₂, and MoO₂ to validate our approach and to study the reactivity of the Mo atom. For these systems we observed spin flips as a consequence of a charge transfer process. The Mo atom is always the electron donor. For MoN₂ we found, after two spin flips, the thermodynamically unstable side-on complex as the product of the reaction. For MoO₂, the O₂ molecule is completely dissociated after two spin flips, and the Mo–O bonds are formed. A comparison and explanation of the experimental results is given. We also present a detailed study of the molecular orbitals and spin densities which could be useful for future studies of these systems.

Computational Details

The program packages deMon-KS²⁵ and deMon-properties²⁶ were used to perform all the calculations. The Linear Combination of Gaussian-Type Orbitals–Kohn–Sham–Density Functional Theory (LCGTO-KSDFT) method is implemented in this program. The local spin-density approximation (LSDA) of Density-Functional-Theory (DFT) was included as in Vosko, Wilk, and Nusair²⁷ while the Generalized Gradient Approximation (GGA) calculations used the gradient terms of Perdew and Wang for exchange²⁸ and Perdew for correlation.^{29,30} Full geometry optimization was performed at the LSDA level and the GGA potential was included self consistently for the final energy evaluation.

The Gaussian orbital basis sets³¹ that we have used are (633321/53211*/531+) for molybdenum, (41) for hydrogen, (621/41/1*) for nitrogen, and (621/41/1*) for oxygen. The auxiliary function set used to fit the charge density and the exchange-correlation potential is (5,5;5,5) for molybdenum, (4;4) for hydrogen, (4,3;4,3) for nitrogen, and (4,3;4,3) for oxygen. In this notation, the charge density and the exchange-correlation auxiliary function sets are separated by a semicolon. Following the notation (*k*₁,*k*₂; *l*₁,*l*₂), the number of s-type Gaussians for the charge density (exchange-correlation) fit is represented by *k*₁ (*l*₁), while *k*₂ (*l*₂) gives the number of s- p- and d-type Gaussians in the charge density (exchange-correlation) auxiliary function set. To study the influence of polarization functions on the hydrogen atoms, we also used a (41/1*) basis set in combination with a (4,1;4,1) auxiliary function set for the H atom. Our calculations showed that the contribution of the polarization functions in the MOs of the MoH₂ as well as the Mulliken population of these functions are negligible.

TABLE 1: Some Electronic Configurations of the Mo Atom and Their Energies Relative to the Ground State. Our Results at the LSDA Level (Vosko, Wilk, and Nusair²⁷) and at the GGA Level (Perdew and Wang for Exchange²⁸ and Perdew for Correlation^{29,30}) Compared to Experimental Data⁷ and Available CI Results¹⁸

atomic configuration of Mo	ΔE (kcal/mol)			
	EXP ^a	CI ^b	LSDA	GGA
4d ⁵ 5s ¹ (⁷ S)	0.0	0.0	0.0	0.0
4d ³ 5s ¹ (⁵ S)	30.80	33.45	28.87	25.79
4d ⁵ 5s ¹ (⁵ D)	57.69	61.62	54.62	55.49

^a Experimental data from ref 35. ^b MRSDCI calculations were done using multireference singles and doubles by Li and Balasubramanian, ref 18.

The charge density was fitted analytically, while the exchange-correlation potential was fitted numerically on a grid³² (deMon option FINE)²⁵ comprised of 32 radial shells and 26 angular points per shell.³² At the end of each SCF procedure, the exchange-correlation contribution to the energy gradients were calculated by numerical integration on an augmented set of grid points consisting of the same 32 radial shells with 50, 110, or 194 angular grid points.

Full geometry optimization without symmetry constraints have been performed, starting from several initial geometries to locate different minima on the potential energy surface (PES). Geometries were optimized using the method of Broyden-Fletcher-Goldfarb-Shanno (BFGS)³³ or the conjugate gradient method.

In order to discriminate minima from other critical points on the potential energy surface, a vibrational analysis was performed using numerical differentiation (two-point finite differences) of the gradients, using a displacement (GSTP) equal to 0.02 au and a density convergence threshold equal to 10⁻⁶. The effects of the GSTP and the density convergence threshold in vibrational analyses have been discussed elsewhere.³⁴ Since the geometries were optimized at the local level, the vibrations were calculated in the LSDA approximation too. The total energies (available on request) include the nonlocal gradient corrections.

Results and Discussion

This section is organized into three subsections. Section A discusses the comparison of some of our results with other available experimental and theoretical values. Since in this work we performed nonrelativistic density functional calculations, it is important to assure that the relativistic effects are not important for the qualitative description of the studied reactions (except, as already noted, for the important role of spin-orbit coupling in intersystem crossing). We used MoH₂ for this test because accurate relativistic MRSDCI results are available in the literature.¹⁸ Sections B and C describe our results of the geometry optimization of MoN₂ and MoO₂. In section D we present molecular orbital diagrams and spin densities for MoN₂ and MoO₂ and we discuss the nature of the bonding in these molecules.

A. Geometry Optimization of MoH₂. In Table 1, we present some selected electronic configurations of the Mo atom and their relative energy differences to the ground state. We compare our results at LSDA and GGA levels with experimental data.³⁵ The electronic ground state configuration (d⁵s¹) that we found is the same as the experimental one. The calculated energy differences relative to the ⁷S ground state are all smaller than the experimental ones. The error lies between 2 and 5 kcal/mol. This error is small enough for a reliable assignment of the atomic states of the Mo atom. In this table, we also compare with CI calculations reported by Li and Balasubra-

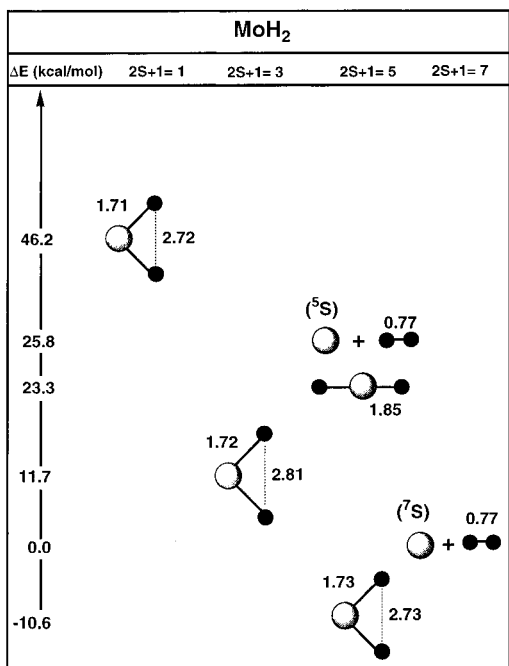


Figure 1. Optimized geometries of MoH₂ for different spin multiplicities. The geometries were obtained at the LSDA level (Vosko, Wilk, and Nusair²⁷), by minimization of the total energy, without symmetry constraints. Bond distances (in Å) and energy differences (in kcal/mol) at the GGA level (Perdew and Wang for exchange²⁸ and Perdew for correlation^{29,30}) are also shown. The GGA results are single-point calculations with the geometry optimized at the LSDA level.

manian.¹⁸ They used relativistic effective core potentials and an MRSDCI in their calculations. In Table 1 we see that the CI energy differences between the atomic states are all larger than the experimental ones. The error of the CI calculations and of our calculations are in the same acceptable range with respect to experiment.

In Figure 1, we present our optimized geometries for MoH₂. As discussed above, these geometries are fully optimized at the LSDA level. Bond distances at the LSDA level and energy differences at the GGA level with respect to Mo(⁷S) + H₂ are also shown. For MoH₂ the most stable spin multiplicity is the

TABLE 2: Our Results and Available CI Results for the Ground State Optimized Geometry of MoH₂. The Energy Differences Are with Respect to Mo(⁷S) + H₂

state	CI		LSDA		ΔE^a (kcal/mol)		
	R_c (Å)	θ_c (deg)	R_c (Å)	θ_c (deg)	CI ^b	LSDA	GGA
⁵ B ₁ ^c	1.67	116	1.72	105	-6.9	-16.56	-10.64

^a Energy differences with respect to Mo(⁷S) + H₂. ^b MRSDCI calculations were done using multireferences singles and doubles by Li and Balasubramanian, ref 18. ^c Note that our choice of axes interchanges the labels B₁ and B₂ with respect to the choice of ref 18.

quintet, which lies 10.6 kcal/mol under the dissociation limit of the separated ⁷S Mo atom and the H₂. The formation of two Mo–H bonds has reduced the multiplicity; the magnetic moment of the system is reduced by 2 μ_B (see ref 36 for other examples of the interplay between chemisorption and magnetism). The ground state is a bent structure, where the H₂ molecule is completely dissociated. We find also bent minima on the singlet and the triplet PES, however these states are less stable than the quintet and lie 11.7 and 46.4 kcal/mol (triplet and singlet, respectively) above the dissociation limit.

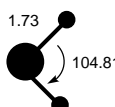
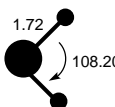
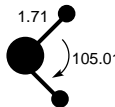
Also for comparison, in Table 2 we compare the ground state optimized geometry of MoH₂ with available CI results. The optimized geometry LSDA has a longer bond distance and a smaller bond angle than the CI geometry. This could be due to relativistic effects, to residual correlation errors, or to a combination of these. However, for a qualitative description of the reactivity of the Mo atom with small molecules, these rather small differences are not crucial. The energy differences reported in Table 2 are with respect to Mo(⁷S) + H₂. For the ⁵B₁ ground state,¹ the Kohn–Sham electronic configuration is identical with the predominant configuration in the CI. In Figure 1, one can also see that there is no linear minimum below the dissociation limit and there is no bent minimum on the septet potential energy surface. These results are in agreement with the CI calculations.

In Table 3, molecular structures, symmetry point groups, electronic states, relative energies at LSDA and GGA levels, and electronic configurations of the most stable geometries of triplet, quintet, and septet states are summarized. We also

TABLE 3: Molecular Structures, Symmetry Point Groups, Electronic States, Relative Energies at the LSDA Level (Vosko, Wilk, and Nusair²⁷) and at the GGA Level (Perdew and Wang for Exchange²⁸ and Perdew for Correlation^{29,30}), and Electronic Configuration of the Most Stable Geometries of Septet, Quintet, Triplet, and Singlet Spin States of MoH₂. The GGA Results Are Single-Point Calculations with the Geometry Optimized at the LSDA Level. For Comparison, Available CI Energy Differences¹⁸ Are Listed, Too

structure	point group	state	ΔE (kcal/mol)			configuration
			CI	LSDA	GGA	
	C_{2v}	⁵ B ₁	-6.90	-18.29	-10.64	$b_1^2 a_1^2 b_2^1 a_1^1 a_2^1 a_1^1$
		Mo(⁷ S) + H ₂ (¹ Σ_g^+)	0.0	0.0	0.0	
	C_{2v}	³ B ₁	27.0	4.81	11.69	$a_1^2 b_1^2 a_1^2 a_2^1 b_2^1$
	$D_{\infty h}$	⁵ Σ_g^+	16.60	19.38	23.34	$\sigma_g^2 \sigma_u^2 \delta_g^1 \delta_g^1 \pi_g^1 \pi_g^1$
		Mo(⁵ S) + H ₂ (¹ Σ_g^+)	33.45	28.87	25.79	
	C_{2v}	singlet	41.0	33.50	46.16	

TABLE 4: Molecular Structure, Electronic Ground States, and Harmonic Frequencies (in inverse centimeters) of the Quintet, Triplet, and Singlet States of MoH₂. All Vibrational Studies Were Performed at the LSDA Level (Vosko, Wilk, and Nusair²⁷)

structure	state	harmonic frequencies	assignment
	⁵ B ₁	419 1778 1793	a ₁ b ₁ a ₁
	³ B ₁	493 1823 1834	a ₁ b ₁ a ₁
	singlet	421 1812 1842	a ₁ a ₁ a ₁

present the CI energy differences. For the quintet ground state, the GGA energy difference is around 4 kcal/mol more stabilizing than the CI value. The next quintet, the linear structure, ⁵Σ_g state, is at 23.3 kcal/mol above the dissociation limit (Mo (⁷S) + H₂). For this excited quintet state, the difference between the CI and the GGA values is around 7 kcal/mol. Unfortunately, there are no experimental results for these systems. However, if we consider the errors with respect to the experimental values for the Mo atom in Table 1, we can expect that our results are not far away from the experimental ones. The linear quintet structure lies under the quintet dissociation limit. The same result is found with the CI calculations. All these results indicate that the GGA values are in reasonable agreement with the CI results for the quintet states.

In Figure 1 and in Table 3, we also report the lowest triplet structure that we found. This is a bent ³B₁ state which lies at 11.7 kcal/mol above the dissociation limit. In the CI calculations, three triplets were found between 27 and 34 kcal/mol above the dissociation limit. During our optimization of the bent ³B₁ state, we first used fractional occupation of the orbitals in order to obtain SCF convergence. We found a structure, 31 kcal/mol above the dissociation limit, with the same geometry and with four fractionally occupied orbitals. Comparing this value with the CI result that we also present in Table 3 for this ³B₁ state, we can see that the value for this “average” state fits well with the CI calculations that we are using in the comparison. However when we improved the calculation, we obtained the above mentioned ³B₁ state with integer occupation numbers. Further investigation of both theoretical approaches would be necessary to clarify this situation.

In Figure 1 and Table 3 we see that the lowest singlet state that we found is a bent structure. When this geometry was optimized, we used fractional occupation numbers in order to obtain convergence. We did not try to get integer occupation numbers for this system because it is a highly excited state that lies 46.2 kcal/mol above the dissociation limit. For this reason we cannot assign the electronic state. This energy difference is quite close to the results of the CI calculations, and the geometries are very similar.

We verified that the optimized geometries are minima by performing vibrational analyses. In Table 4 we report results for the most stable structures of the quintet, triplet, and singlet. The calculated frequencies indicate that all the structures have similar metal–hydrogen bonding. To a first approximation the differences in the electronic structure of these systems involve

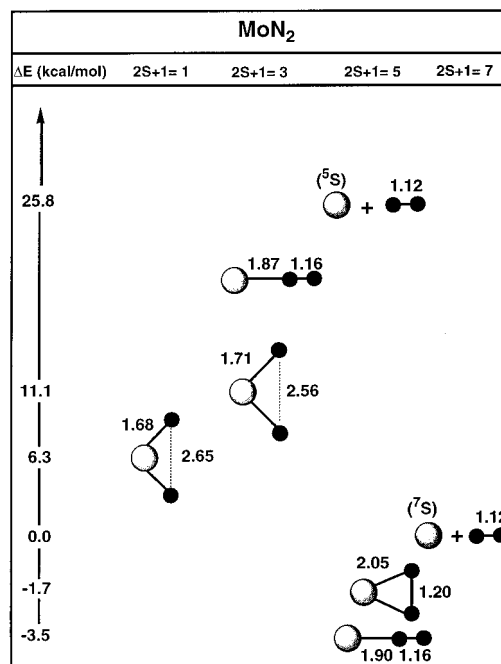


Figure 2. Optimized geometries of MoN₂ for different spin multiplicities. The geometries were obtained at the LSDA level (Vosko, Wilk, and Nusair²⁷), by minimization of the total energy, without symmetry constraints. Bond distances (in Å) and energy differences (in kcal/mol) at the GGA level (Perdew and Wang for exchange²⁸ and Perdew for correlation^{29,30}) are also shown. The GGA results are single-point calculations with the geometry optimized at the LSDA level.

changes in the spin state of the Mo atom only. Essentially nonbonding orbitals are involved which results in similar sets of harmonic frequencies.

As we can see from this comparison, our results are overall in good agreement with the experimental (for the atom) and relativistic CI values reported before.¹⁸ The (scalar) relativistic effects are not crucial for a qualitative description of these reactions, and we can use this methodology in order to explain the experimental behavior. Within the density functional theory, we can study the reactivity of transition metal atoms, using the optimized geometries and the vibrational analysis calculations at the LSDA level. It is relevant to test different initial geometries with different spin multiplicities during the geometry optimization procedure. For the final energy evaluation, it is important to include the GGA corrections.

B. Geometry Optimization of MoN₂. The optimized geometries of MoN₂ are shown in Figure 2. We started from several initial geometries and multiplicities and we found several critical points on the different PES. Bond distances at the LSDA level and GGA energy differences with respect to the dissociation limit (Mo (⁷S) + N₂) are also shown.

For the septet states, no minima were found. For the quintet states, Figure 2 and Table 5 show two different minima with similar stability, the linear and the bent structures, both with the N₂ molecularly bonded to the Mo atom. We can see immediately that the bonding is different from the MoH₂ system, since the energy difference for MoN₂ with respect to the dissociation limit is very small (−3.5 and −1.7 kcal/mol for the linear and the bent structures respectively). These energies fall into the “weak interaction” category, similar to the energies of the hydrogen bond or Mulliken charge transfer complexes³⁸ and, contrary to the case of strongly bond systems,^{39,40} may not be reliable even at the GGA level. There is still a tendency to overbind such situations with currently available functionals. Hence, we are not overly concerned that the experimental results⁸ showed no reactivity of Mo with N₂. A quantitative treatment must await the development of improved functionals.

TABLE 5: Molecular Structures, Symmetry Point Groups, Electronic States, Relative Energies at the LSDA Level (Vosko, Wilk, and Nusair²⁷) and at the GGA Level (Perdew and Wang for Exchange²⁸ and Perdew for Correlation^{29,30}), and Electronic Configuration of the Most Stable Geometries of Septet, Quintet, Triplet, and Singlet Spin States of MoN₂. The GGA Results Are Single-Point Calculations with the Geometry Optimized at the LSDA Level

structure	point group	state	ΔE (kcal/mol)		configuration
			LSDA	GGA	
	$C_{\infty v}$	5Π	-20.06	-3.47	$\sigma^2\pi^2\pi^1\delta^1\sigma^1$
	C_{2v}	$5B_1$	-19.20	-1.67	$a_1^2 b_1^2 a_2^1 a_1^1 b_2^1 a_1^1$
		Mo ($7S$) + N ₂ ($1\Sigma_g^+$)	0.0	0.0	
	C_{2v}	$1A_1$	-20.10	6.29	$a_2^2 b_2^2 a_2^1 b_1^2$
	C_{2v}	$3B_1$	-10.66	11.11	$a_2^2 b_2^2 a_2^1 b_1^1 a_1^1$

In Figure 2 and Table 5 we can see that the dissociation limit on the quintet PES (Mo ($5S$) + N₂) is 25.8 kcal/mol less stable than the dissociation limit on the septet PES (Mo ($7S$) + N₂). On the singlet and the triplet PES, we found bent minima with the N₂ molecule completely dissociated. These structures are thermodynamically unstable with respect to the septet dissociation limit but stable with respect to the quintet dissociation limit. Hence, the reaction between Mo and N₂ leading to a metastable triplet or singlet could be possible, if the Mo atom is in an excited quintet state.

In Table 6, we present the LSDA vibrational harmonic frequencies of the most stable structures of MoN₂ with different multiplicities. We also present the harmonic frequency of the N₂ molecule for comparison. As we can see in this table, the experimental value of the N₂ stretching frequency is 2358.57 cm⁻¹⁴¹ and the LSDA value is 2363 cm⁻¹, in good agreement. Table 6 shows that the vibrational harmonic frequencies are positive, indicating that the structures are minima on the different PES. The calculated frequencies could help guide future experimental characterization of some of these states, if they can be isolated. We note that the N–N bond distances as well as the highest frequencies of these structures indicate that the N–N bond is weakened from the first to the last structure in Table 5.

C. Geometry Optimization of MoO₂. The optimized geometries of MoO₂ are shown in Figure 3. We started from several initial geometries and multiplicities and we found several critical points on the different PES. Bond distances at the local level and energy differences at the nonlocal level with respect to the dissociation limit (Mo ($7S$) + O₂) are also shown.

In contrast with MoN₂, for MoO₂ we can see in Figure 3 that we found many local minima which are thermodynamically stable. For the nonet state no minima were found, so we will exclude this PES from the following discussion. The ground state is a triplet bent structure which has a binding energy of 144 kcal/mol. In further contrast with MoN₂, all of the most stable structures of MoO₂ have lost the covalent O–O bond, in favor of Mo–O bonding (whereas the N–N bond remained intact for the most stable structures of MoN₂).

The bent structure is the most stable structure on all PES. The ground state is a triplet followed by a singlet and a quintet. Comparing the singlet, the triplet and the quintet bent structures,

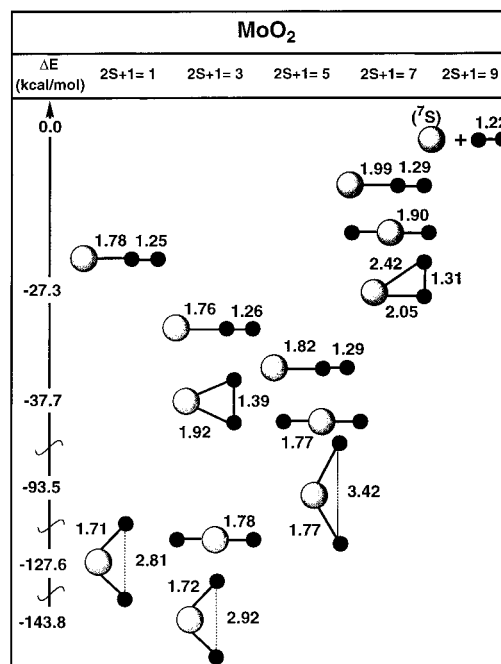





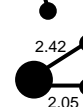

Figure 3. Optimized geometries of MoO₂ for different spin multiplicities. The geometries were obtained at the LSDA level (Vosko, Wilk, and Nusair²⁷), by minimization of the total energy, without symmetry constraints. Bond distances (in Å) and energy differences (in kcal/mol) at the GGA level (Perdew and Wang for exchange²⁸ and Perdew for correlation^{29,30}) are also shown. The GGA results are single-point calculations with the geometry optimized at the LSDA level.

TABLE 6: Molecular Structure, Electronic Ground State, and Harmonic Frequencies (in inverse centimeters) of the Quintet, Triplet, and Singlet States of MoN₂. For Comparison, the Experimental and the Calculated Harmonic Frequency of N₂ Is Also Reported. All Vibrational Studies Were Performed at the LSDA Level (Vosko, Wilk, and Nusair²⁷)

structure	state	harmonic frequencies	assignment
	5Π	322 505 2003	π σ^+ σ^+
	$5B_1$	427 477 1748	a_1 b_1 a_1
	$1A_1$	469 990 1078	a_1 b_1 a_1
	$3B_1$	347 814 1032	a_1 b_1 a_1
	$1\Sigma_g^+$	2363 (2358.57)	

we can see that the Mo–O bond distance is similar, but the O–O bond length increases with the multiplicity. In this case, it seems that the molecular orbitals of the O₂ molecule are affected by the exchange of spin multiplicities. The covalent bonds between the Mo atom and the oxygen atoms are formed while the spins pair up, reducing the overall multiplicity. The effect of chemisorption on the metal magnetism has also been

TABLE 7: Molecular Structures, Symmetry Point Groups, Electronic States, Relative Energies at the LSDA Level (Vosko, Wilk, and Nusair²⁷) and at the GGA Level (Perdew and Wang for Exchange²⁸ and Perdew for Correlation^{29,30}), and Electronic Configuration of the Most Stable Geometries of Septet, Quintet, Triplet, and Singlet Spin States of MoO₂. The GGA Results Are Single-Point Calculations with the Geometry Optimized at the LSDA Level

structure	point group	state	ΔE (kcal/mol)		configuration
			LSDA	GGA	
	C_{2v}	3B_2	-164.83	-143.75	$b_2^2 a_1^2 b_1^2 a_1^1 b_2^1$
	C_{2v}	1A_1	-151.43	-127.56	
	C_{2v}	5A_1	-106.07	-93.54	$b_1^2 b_2^2 b_2^1 a_1^1 b_2^1 a_1^1$
	C_s	$^7A''$	-36.00	-27.28	$a_{oo}^2 a_o^1 a_o^1 a_{oo}^1 a_o^1 a_o^1 a_o^1$
	$C_{\infty v}$	Mo (7S) + O ₂ ($^3\Sigma_g^-$)	0.0	0.0	

studied by Fournier *et al.*³⁶. For example, they reported that the addition of the carbon atom reduces the spin magnetic moment of pure nickel by either 2 or 4 μ_B depending on the system.

In Figure 3, we can see that the septet bent structure is completely distorted. The O—O bond distance is longer than the O—O bond distance of the isolated molecule, but it is not dissociated. We will explain the distortion of this structure with the molecular orbitals in the next section.

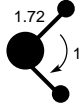
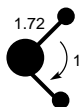

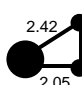
On the triplet PES, another bent minimum with molecularly bound O₂ lies between the two linear structures $D_{\infty h}$ and $C_{\infty v}$. The GGA energy difference between the two bent triplet structures (molecular and dissociative) is 106 kcal/mol. This result indicates that the dissociative reaction of O₂ with the Mo atom is strongly preferred over the molecular adsorption.

For all PES with different spin multiplicities that we studied, the general behavior is that the linear structures are less stable than the bent structures.

In Table 7 we summarize the information for MoO₂. We can see that the stability order is the same at LSDA and GGA levels. The C_{2v} structures are the most stable ones for the singlet, the triplet, and the quintet PES. For the septet spin state, the most stable structure has C_s symmetry. All the structures are thermodynamically stable. The energy difference with respect to the dissociation limit (Mo (7S) + O₂) is very large for all the C_{2v} structures that we present in Figure 3 and Table 7. For the distorted septet, the energy difference is not as large as for the other triangular structures.

In Table 8 we present the vibrational analysis for the most stable MoO₂ structures. The geometry is almost the same for the singlet and the triplet, and the vibrational analysis is in agreement with that. For the quintet the O—O bond length is longer than in the other two states and the vibrational analysis reflects this difference. The smallest normal mode of the quintet is bigger than the smallest normal modes of the singlet and the triplet. Furthermore, for the singlet and the triplet, the other two frequencies are very close to each other, while for the quintet they are separated. For the septet bent structure, the normal modes of vibration indicate that the two Mo—O bond distances are different. We hope that this information will be useful for future experimental investigations.

TABLE 8: Molecular Structure, Electronic Ground State, and Harmonic Frequencies (in inverse centimeters) of the Septet, Quintet, Triplet, and Singlet States of MoO₂. All Vibrational Studies Were Performed at the LSDA Level (Vosko, Wilk, and Nusair²⁷)

structure	state	harmonic frequencies	assignment
	3B_2	264 936 967	a_1 b_1 a_1
	1A_1	238 936 982	a_1 b_1 a_1
	5A_1	539 679 835	a_1 b_1 a_1
	$^7A''$	233 512 1204	a' a' a'

In this section we presented the geometry optimization of MoN₂ and MoO₂. We found several differences between these two systems. For MoO₂ all the optimized structures are more stable than the dissociation limit, while for MoN₂ only two structures lie beneath the dissociation limit. In Figures 2 and 3 we also can see that the dissociation energies of the MoN₂ stable structures are very small, while for MoO₂ they are very large. Thermodynamically, MoO₂ is very stable while MoN₂ is not. This is consistent with the experimental results of Lian *et al.*⁸, who found no reactivity between Mo and N₂ and large reactivity between Mo and O₂. We will explain the different bond situation with molecular orbital diagrams, and we will propose a possible reaction mechanism in the next section.

D. Molecular Orbitals and Spin Densities. In order to

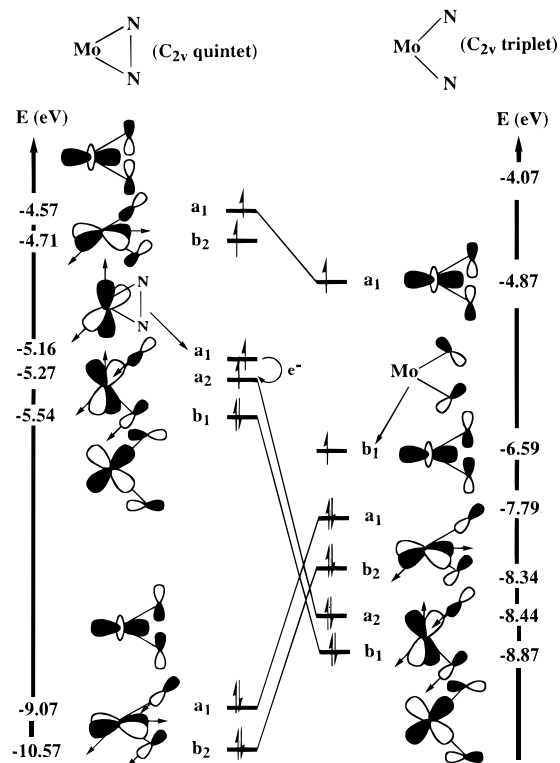


Figure 4. Molecular orbital correlation diagram of MoN_2 (quintet to triplet) with C_{2v} symmetry. Orbital symmetries and eigenvalues (in eV) at the GGA level (Perdew and Wang for exchange²⁸ and Perdew for correlation^{29,30}) are presented. The GGA results are single-point calculations with the geometry optimized at the LSDA level. The spin flip is indicated by an arrow in the orbital diagram of the quintet.

explain the reaction between the Mo atom and these small molecules, we have analyzed the molecular orbital diagrams. The first step of the reaction between the Mo atom and the N_2 molecule can formally be viewed as the transfer of an α electron from the Mo atom into an antibonding orbital of the N_2 . This charge transfer is connected with a spin flip, changing the multiplicity of the system from a septet to a quintet. The Mo atom can only react as an electron donor because the electron pairing on the Mo atom is energetically unfavorable due to the coulombic interaction. The behavior of the Mo atom to avoid electron pairing manifests itself in the states of the low-lying atomic configurations as well as in the experimental observation,⁸ since Mo atoms show no reactivity toward electron donors like NH_3 . This first electron transfer to N_2 cannot break the

strong N–N bond, and the reaction is a weak adsorption between Mo and N_2 on the quintet surface.

In Figure 4, we present the molecular orbital correlation diagram of the MoN_2 (quintet to triplet) with C_{2v} symmetry. The N_2 molecule is not dissociated in the quintet state but it is in the triplet, as can be seen in Figure 2 and Table 5. When we change from the quintet to the triplet, we can see the stabilization of the N–N antibonding and the destabilization of the N–N bonding orbitals. The second step of the reaction occurs when another α electron is formally transferred, with a change in the multiplicity from quintet to triplet. In the quintet, there is a nonbonding a_1 orbital (at 5.16 eV) on the Mo atom that lies only 0.11 eV above an a_2 orbital. The a_2 orbital is bonding in the Mo–N bond and antibonding in the N–N bond. The charge transfer goes from the a_1 nonbonding orbital into the a_2 orbital, as we indicate in Figure 4. As a consequence of this charge transfer to a π^* antibonding orbital of N_2 , the N–N bond is weakened. Because this orbital is also a bonding Mo–N orbital, the charge transfer generates covalent Mo–N bonds too. However, this second electron transfer is thermodynamically unstable, as Figure 2 and Table 5 indicate. Figure 4 shows that the highest b_2 orbital of the quintet is replaced by a b_1 orbital of the triplet. From our calculation we are not able to follow this orbital exchange because we have only optimized minima structures on the triplet and quintet PES. The charge transfer from the Mo atom to the N_2 molecule is the main process. The first electron that is transferred generates a weak adsorption between Mo and N_2 . The second electron that is transferred weakens the N–N bond and induces the dissociation of the molecule. The weak adsorption and the dissociation of N_2 seems to be a two-step process with an electron transfer from Mo to N_2 that is connected with a spin flip. However, this process is thermodynamically unfavorable.

In Figures 5 and 6, we present spin density plots of the triangular quintet state and triplet state of MoN_2 , respectively. We indicate in each figure the position of the atoms. In the MoN_2 quintet, the negative spin density is distributed over the whole N_2 molecule in an antibonding π^* orbital (b_1 orbital in Figure 4). The spin flip from the quintet to the triplet changes the spin density, since in the triplet state the unpaired electrons are delocalized over the whole system, as can be seen in Figure 6. The α spin density is now distributed over the whole covalently bonded system. This new distribution of the spin density is mostly due to the new singly occupied b_1 orbital in the triplet state (see Figure 4).

In the reaction of the Mo atom with O_2 , the first step is a

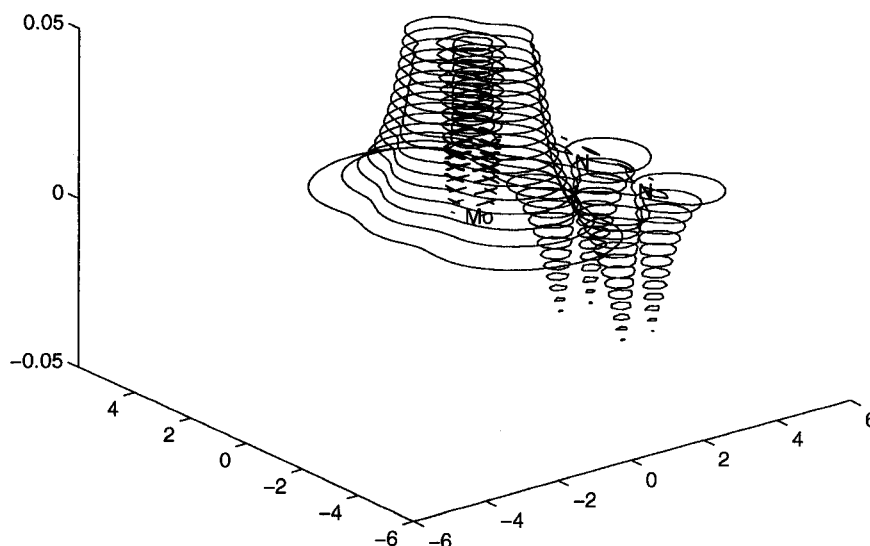


Figure 5. Spin density plot of the triangular MoN_2 quintet state. All values are in atomic units.

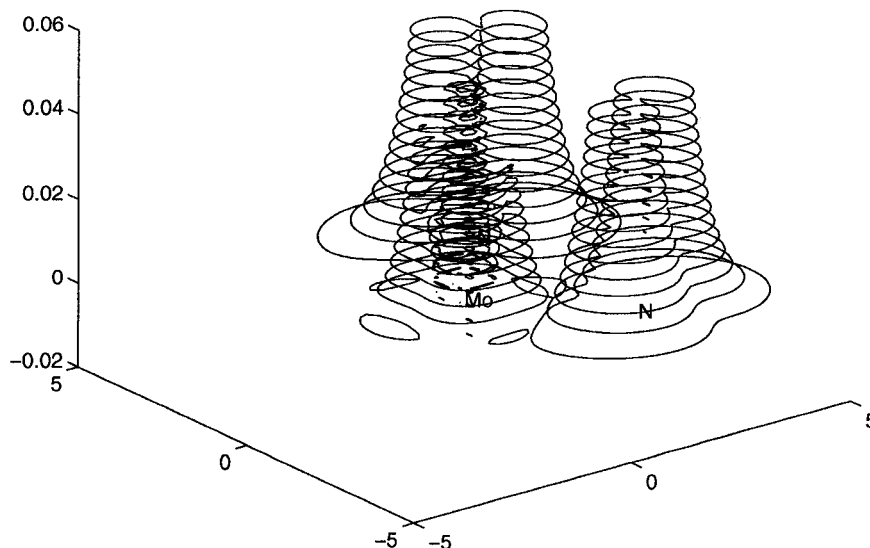


Figure 6. Spin density plot of the triangular MoN₂ triplet state. All values are in atomic units.

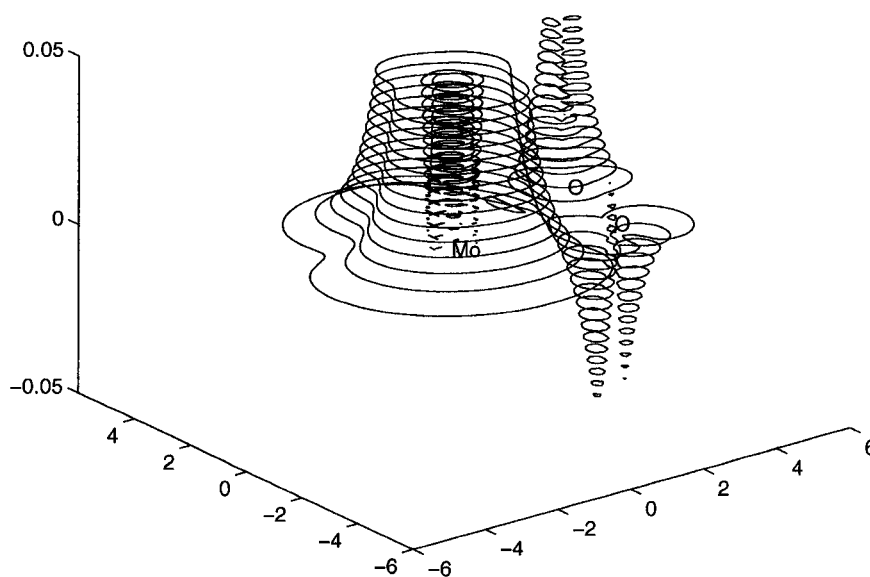


Figure 7. Spin density plot of the C_s MoO₂ septet state. All values are in atomic units.

weak adsorption of the O₂ (triplet) on the Mo atom on the septet surface. This first step of the reaction occurs when an α electron is formally transferred from the Mo atom into the antibonding π^* system of the O₂. The electron transfer is connected with a spin flip, which changes the multiplicity from a nonet to a septet. Contrary to the previously discussed reaction of Mo with N₂, the first charge transfer step in the reaction of the Mo with O₂ stabilizes the system considerably and breaks the C_{2v} symmetry. The break in the symmetry can be easily understood when one looks at the spin density of the septet system (Figure 7). One oxygen atom has positive and the other negative spin density. The reason for these different spin densities on the oxygen atoms lies in the charge transfer from the Mo atom into the partially filled antibonding π^* system of the O₂ molecule.

In Figures 8 and 9, we present the molecular orbital diagrams of the most stable MoO₂ structures on the septet, quintet, and triplet PES of MoO₂. When we compare the molecular orbital diagram of the MoO₂ septet (Figure 8, left side) with that of the MoN₂ quintet (Figure 4, left side) we see a very similar structure in the order of the molecular orbitals. The lowest lying molecular orbitals are bonding between the Mo atom and the molecule and bonding in the molecule. The next class of molecular orbitals is bonding between the Mo and the molecule and antibonding in the molecule. After these orbitals we find more or less nonbonding orbitals. The highest occupied orbitals

are antibonding between the Mo atom and the molecule, and antibonding within the molecule. Comparing the septet and the quintet minimum of MoO₂ (Figure 8, right side), one can see several differences with the correlation diagram of MoN₂. First, the correspondence of septet and quintet orbitals is more difficult for the MoO₂ system than for the MoN₂ system. More importantly, the classification of the orbitals changes due to the change in the geometry. As an example, we find that the highest occupied orbital of the MoO₂ septet is antibonding between Mo and O₂ and antibonding in the O₂. From the orbital topography we assign this orbital to the lowest orbital of the MoO₂ quintet that we present in Figure 8. The explanation for this shift of the orbital is the fact that the antibonding δ -type orbital from the side-on complex of the MoO₂ septet changes to a bonding π -type orbital in the MoO₂ quintet. This change of side-on complex orbitals to Mo–O bonding orbitals is the reason for the energetic stabilization of the MoO₂ quintet compared with the septet. In the MoN₂ system, this mechanism is not working because the N–N bond is not dissociated even in the triplet state. From the orbital picture we see that the MoN₂ triplet is still a side-on complex. In Figure 9 the molecular orbital correlation diagram from the MoO₂ quintet to the triplet ground state is presented. The topography of the orbitals changes only little from the quintet to the triplet. However, some π bonding between the oxygens in the quintet is substituted by σ bonding

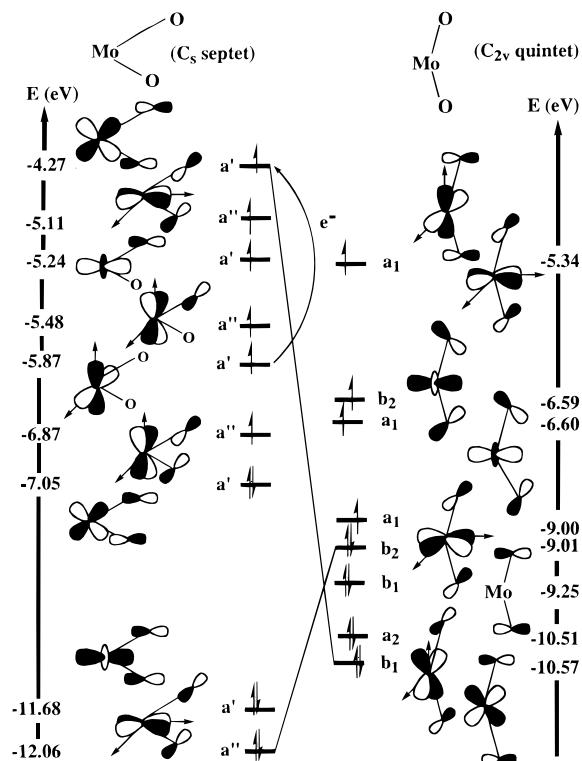


Figure 8. Molecular orbital correlation diagram of the MoO₂ (septet to quintet) with C_s and C_{2v} symmetry, respectively. Orbital symmetries and eigenvalues (in eV) at the GGA level (Perdew and Wang for exchange²⁸ and Perdew for correlation^{29,30}) are presented. The GGA results are single-point calculations with the geometry optimized at the LSDA level.

in the triplet. This change of bonding results in a shorter distance between the two oxygen atoms in the triplet compared to the quintet.

In Figure 10 we present the spin density distribution in the MoO₂ quintet. Similar to the MoN₂ triplet, the α spin density is distributed over the whole molecule.

Summary and Conclusions

In this paper, we presented a density functional study of the reaction between a Mo atom and H₂, N₂, and O₂. We used MoH₂ to validate the DFT methodology, comparing with accurate relativistic CI results. From this comparison, we can see that DFT methods are suitable for the study of this system

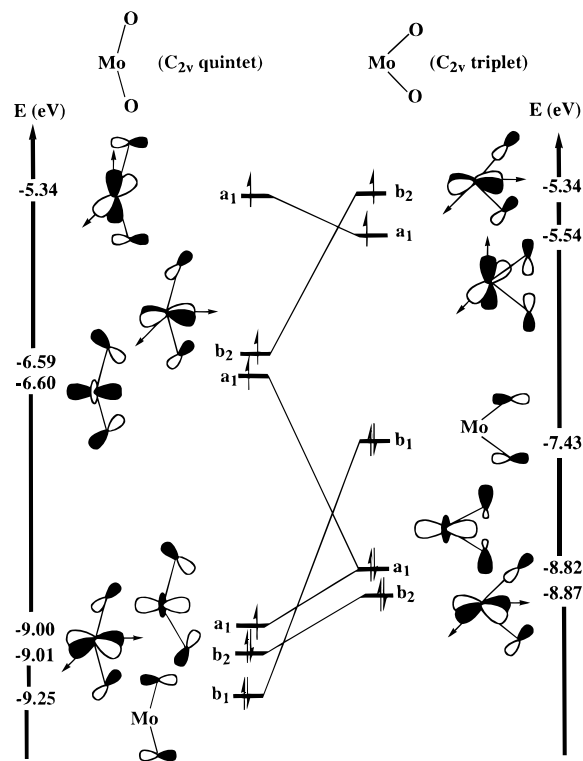


Figure 9. Molecular orbital correlation diagram of the MoO₂ (quintet to triplet) with C_{2v} symmetry. Orbital symmetries and eigenvalues (in eV) at the GGA level (Perdew and Wang for exchange²⁸ and Perdew for correlation^{29,30}) are presented. The GGA results are single-point calculations with the geometry optimized at the LSDA level.

and that the scalar relativistic effects are not crucial for a qualitative descriptions of these reactions. For the geometry optimization, the local exchange-correlation potentials can be used. As already is well-known, GGA potentials must be used to obtain the correct energetic order of the optimized MoH₂ structures.

After this validation of the methodology, we studied the reactions of a Mo atom with N₂ and O₂ in order to obtain an explanation of the different observed reactivities. For this study, we scanned the different PES of these reactions to find local minima. For MoN₂ we found only two local minima under the dissociation limit on the quintet surface. Both structures, linear and bent, are very weakly bonded, and caution is required.

For MoO₂ we found several local minima on the septet,

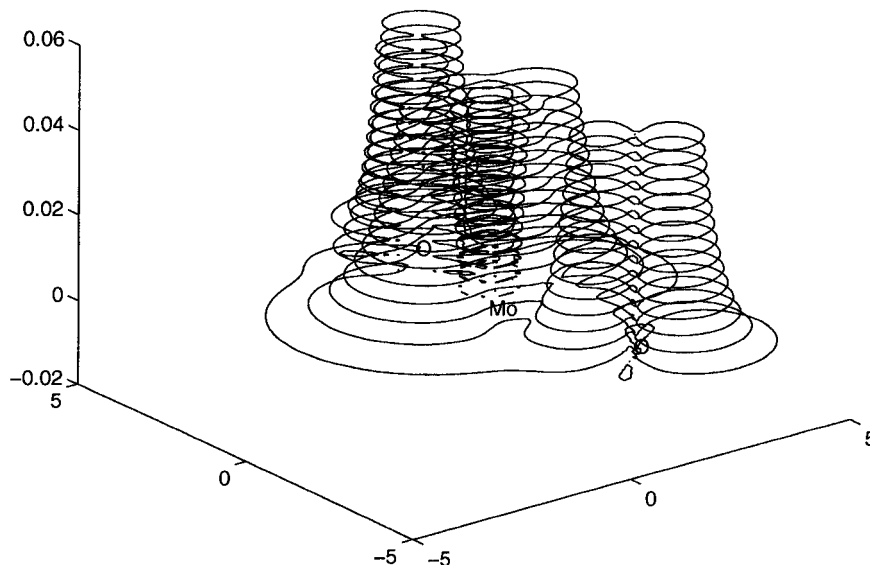


Figure 10. Spin density plot of the C_{2v} MoO₂ quintet state. All values are in atomic units.

quintet, triplet, and singlet PES, which are thermodynamically stable. The lowest minimum that we found is a bent structure on the triplet PES. For this system, we suggest a two-step reaction path, which goes over the bent minimum on the septet PES to the bent minimum on the quintet one. This structure can be stabilized in a following step, changing from the quintet to the triplet bent structure. The breaking of the C_{2v} symmetry in the septet minimum is very interesting. The analysis of the spin density and the molecular orbitals shows that this symmetry breaking is due to the partial filling of the antibonding π^* orbital in the O₂ molecule. For the systems that we presented, the covalent bonds are formed while the spins pair up, reducing the overall multiplicity.

From this study, we can see that the different reactivities of N₂ and O₂ with the Mo atom are due to the different bond strengths of these molecules. For the MoO₂ system, the O₂ molecule is completely dissociated after two spin flips, and the Mo–O bonds are formed. For the MoN₂ system, we found the thermodynamically unstable side-on complex as the product of the reaction, even after two spin flips. The Mo atom is always the electron donor in these reactions.

The theoretical explanation of the experimental results that we presented in this paper provide a better understanding of the electronic structure and the reaction mechanism of the Mo atom with H₂, N₂, and O₂.

Acknowledgment. The authors would like to thank Drs. Patrizia Calaminici and Alberto Vela for helpful discussions. We would like to acknowledge the Laboratorio de Supercomputo y Visualización en Paralelo at UAM-Iztapalapa (México) for providing computer time on the Silicon Graphics Power Challenge computer, and to DGSCA/UNAM (México) for providing computer time on the CRAY YMP 4/432. Support from NSERC (Canada) and the VW-Stiftung (Germany) is gratefully acknowledged.

References and Notes

- Hintermann, A.; Manninen, M. *Phys. Rev. B* **1983**, *27*, 7262.
- Ekardt, W. *Phys. Rev. B* **1988**, *37*, 9993.
- Upton, T. H. *Phys. Rev. Lett.* **1986**, *56*, 2168.
- Robles, J.; Iñiguez, M. P.; Alonso, J. A.; Mananes, A. Z. *Phys. D* **1989**, *13*, 269.
- Fournier, R. *Int. J. Quantum. Chem.* **1994**, *52*, 973.
- Geusic, M. E.; Morse, M. D.; Smalley, R. E. *J. Chem. Phys.* **1985**, *82*, 590.
- Morse, M. D.; Geusic, M. E.; Heath, J. R.; Smalley, R. E. *J. Chem. Phys.* **1985**, *82*, 2293.
- Lian, L.; Mitchell, S. A.; Rayner, D. M. *J. Phys. Chem.* **1994**, *98*, 11 637.
- Mitchell, S. A. Personal communication, 1994.
- Siegbahn, P. E. M.; Blomberg, M. R. A.; Bauschlicher, C. W. *J. Chem. Phys.* **1984**, *81*, 1373.
- Ruiz, M. E.; Garcia-Prieto, J.; Novaro, O. *J. Chem. Phys.* **1984**, *80*, 1529.
- Garcia-Prieto, J.; Ruiz, M. E.; Poulain, E.; Ozin, G. A.; Novaro, O. *J. Chem. Phys.* **1984**, *81*, 5920.
- Garcia-Prieto, J.; Ruiz, M. E.; Novaro, O. *J. Am. Chem. Soc.* **1985**, *107*, 5635.
- Novaro, O.; Garcia-Prieto, J.; Poulain, E.; Ruiz, M. E. *J. Mol. Struct.: THEOCHEM* **1986**, *135*, 79.
- Balasubramanian, K. *Chem. Phys. Lett.* **1987**, *135*, 288.
- Balasubramanian, K.; Feng, P. Y.; Liao, M. Z. *J. Chem. Phys.* **1988**, *88*, 6955.
- Balasubramanian, K.; Wang, J. Z. *J. Chem. Phys.* **1989**, *91*, 7761.
- Li, J.; Balasubramanian, K. *J. Phys. Chem.* **1990**, *94*, 545.
- Poulain, E.; Colmenares-Landin, F.; Castillo, S.; Novaro, O. *J. Mol. Struct. THEOCHEM* **1990**, *210*, 337.
- Martinez-Magadan, J. M.; Ramirez-Solis, A.; Novaro, O. *Chem. Phys. Lett.* **1991**, *186*, 107.
- Colmenares-Landin, F.; Castillo, S.; Martinez-Magadan, J. M.; Novaro, O.; Poulain, E. *Chem. Phys. Lett.* **1992**, *189*, 378.
- Sanchez, M.; Ruetter, F.; Hernandez, A. J. *J. Phys. Chem.* **1992**, *96*, 823–828.
- Siegbahn, P. E. M.; Blomberg, M. R. A. *Chem. Phys.* **1984**, *87*, 189.
- Bauschlicher, C. W.; Pettersson, L. G. M.; Siegbahn, P. E. M. *J. Chem. Phys.* **1987**, *87*, 2129.
- DEMON: User's guide, version 1.0 beta, Biosym Technologies: San Diego, 1992.
- Köster, A. M.; Leboeuf, M.; Salahub, D. R. deMon-properties, Université de Montreal, 1995.
- Vosko, S. H.; Wilk, L.; Nusair, M. *Can. J. Phys.* **1980**, *58*, 1200.
- Perdew, J. P.; Wang, Y. *Phys. Rev. B* **1986**, *33*, 8800.
- Perdew, J. P. *Phys. Rev. B* **1986**, *33*, 8822.
- Perdew, J. P. *Phys. Rev. B* **1986**, *34*, 7406E.
- Godbout, N.; Salahub, D. R.; Andzelm, J.; Wimmer, E. *Can. J. Chem.* **1992**, *70*, 560.
- Becke, A. D. *J. Chem. Phys.* **1988**, *88*, 2547.
- Schlegel, H. B. *Ab-initio Methods in Quantum Chemistry-I*; Wiley: New York, 1987.
- Martínez, A.; Vela, A.; Salahub, D. R. *Int. J. Quantum Chem.*, in press.
- Moore, C. E. *Atomic Energy Levels. As Derived from the Analyses of Optical Spectra*; United States Department of Commerce. National Bureau of Standards: Washington, D.C., 1949.
- Fournier, R.; Andzelm, J.; Goursot, A.; Russo, N.; Salahub, D. R. *J. Chem. Phys.* **1995**, *93*, 2919.
- Harris, D. C.; Bertolucci, M. D. *Symmetry and spectroscopy. An introduction to vibrational and electronic spectroscopy.*; Dover Publications: New York, 1989.
- Ruiz, E.; Salahub, D. R.; Vela, A. *J. Am. Chem. Soc.* **1995**, *117*, 1141.
- Salahub, D. R.; Fournier, R.; Mlynarski, P.; Papai, I.; St-Amant, A.; Ushio, J. In *Density Functional Methods in Chemistry*; Labanowski, J., Andzelm, J., Eds.; Springer-Verlag: Berlin, 1991.
- Ziegler, T. *Chem. Rev.* **1991**, *91*, 651.
- Huber, K. P.; Herzberg, G. *Molecular Spectra and Molecular Structure*; Van Nostrand-Reinhold: New York, 1979; Vol 4.